Available online at www.sciencedirect.com
SCIENCE DIRECT
Journal of Geodynamics 41 (2006) 112–118
JOURNAL OF GEODYNAMICS
http://www.elsevier.com/locate/jog

Validation of long-period oceanic tidal models with superconducting gravimeters

Jean-Paul Boy [a,*], Muriel Llubes [b], Richard Ray [c], Jacques Hinderer [a], Nicolas Florsch [d]

[a] *EOST-IPGS (UMR CNRS-ULP 7516), 5 rue René Descartes, 67084 Strasbourg, France*
[b] *LEGOS-UMR5566, 18, Avenue Edouard Belin, 31401 Toulouse, France*
[c] *Space Geodesy Branch, Code 926, NASA Goddard Space Flight Center, Greenbelt, MD 20771, USA*
[d] *UMR 7619 Sisyphe, Université Pierre et Marie Curie, 4 Place Jussieu, 75252 Paris Cedex 05, France*

Accepted 30 August 2005

Abstract

Long gravity records from 18 superconducting gravimeters (SG) are used to estimate ocean tide loading for the monthly (Mm) and fortnightly (Mf) tidal waves. The estimates are compared with predicted ocean loading computed from various global tidal models. Despite their long-term sensitivity, the SG non-tidal noise continuum in the near-monthly band is large and renders the Mm estimates too imprecise for validating the different models. For most SG we are able to demonstrate that recent Mf tidal hydrodynamical models that assimilate satellite altimeter data are in significantly better agreement with SG tidal records than an equilibrium tidal model or the old Schwiderski [Schwiderski, E.W., 1980. On charting global ocean tides. Rev. Geophys. Space Phys. 18 (1), 243–268] model.

Keywords: Superconducting gravimeters; Long-period ocean tides; Ocean tidal loading

1. Introduction

Several previous studies have shown that precise tidal gravity measurements can be used as a validation tool of ocean tidal models in the diurnal and semi-diurnal frequency bands (see, for example, Boy et al., 2003; Baker and Bos, 2003; Bos et al., 2002) as well as higher frequencies (Boy et al., 2004). Very few studies have also shown that they can also be used for validating long-period ocean tides (see, for example, Bos et al., 2000). Due to their high sensitivity and their long time stability (see, for example, Richter et al., 1995) superconducting gravimeters (SG) can be used to study long-period ocean tidal loading (Sato et al., 1997), even for mid-latitude instruments, where the degree 2 zonal potential is lower than for the high latitude regions. We here conduct a analysis similar to our previous work on the major ocean diurnal and semi-diurnal tides (Boy et al., 2003), i.e. by comparing ocean tidal loading observed with about 20 SG and computed from several ocean tidal models for the fortnightly (Mf) and the monthly (Mm) waves.

* Corresponding author.
E-mail address: jpboy@eost.u-strasbg.fr (J.-P. Boy).

0264-3707/$ – see front matter © 2005 Elsevier Ltd. All rights reserved.
doi:10.1016/j.jog.2005.08.026

We present in Section 2 a brief description of the ocean tidal models used in this study, as well as some particular characteristics of Mf and Mm ocean waves. Section 3 is devoted to the processing of SG records. Concluding remarks and discussions are given in Section 4.

2. Long period ocean tides

We use five different long-period ocean tide models in this paper: an equilibrium tide (Agnew and Farrell, 1978), Schwiderski (1980), and three recent models NAO99b (Matsumoto et al., 2000), FES99 (Lefèvre et al., 2002) and TPXO.6 (Egbert and Erofeeva, 2002). The last four models are hydrodynamical solutions with assimilation of tide gauges for Schwiderski, no assimilation for NAO99b, with assimilation of tide gauge and Topex/Poseidon altimetry data for FES99, and an inverse solution of Topex/Poseidon for TPXO.6.

Figs. 1 and 2 show the amplitude and phase lag (referred to Greenwich), respectively, of the fortnightly (Mf), and the monthly (Mm) ocean tides according to four different ocean models. Unlike the higher frequency tides, i.e. in the diurnal and semi-diurnal frequency bands, they differ only slightly from the equilibrium tides (Egbert and Ray, 2003), except for the Mm tide model from Schwiderski (1980).

Ocean tidal loading is computed through a convolution of the tidal sea height variations with a Green's function (see, for example, Farrell, 1972) over the entire ocean surface. We determine the sensitivity of ocean tidal loading estimates, by computing the loading on spherical caps centered on the SG, with increasing angles from a few degrees (we only take into account nearby sea height variations) up to 180° (convolution over the entire Earth surface) (see Boy et al., 2003, for more details). We can conclude (see Fig. 3) that surface gravity measurements are clearly sensitive to global sea height variations (up to distances of 90°).

Mismodelling of ocean tides is only one of the main sources of errors in the estimation of ocean tidal loading effects (see Bos and Baker, 2005). The other large source for coastal stations comes from the accuracy of the coastlines. As some SG (Canberra, Ny Alesund, Syowa and the Japanese instruments) are installed on the vicinity of the seashore, we improve the ocean tidal computation by including a refined land-sea mask extracted from the generic mapping tools (GMT) package (http://gmt.soest.hawaii.edu/).

Tables 1 and 2 show the in-phase and out-of-phase components of the loading computed with several ocean tidal models, for the waves Mm and Mf.

Table 1
In-phase and out-of-phase (nm s^{-2}) ocean tidal loading for five different models and for the monthly wave Mm

	Equilibrium		Schwiderski		FES99		NAO99b		TPXO.6	
	Real	Imaginary	Real	Imaginary	Real	Imaginary	Real	Imaginary	Real	Imaginary
BO	0.03	0.00	0.03	0.09	0.02	0.00	0.02	−0.02	0.03	−0.03
CA	−0.39	0.00	−0.02	0.04	−0.13	0.12	−0.19	0.22	−0.19	0.15
CB	−0.27	0.00	−0.48	0.13	−0.37	−0.01	−0.34	−0.09	−0.33	−0.08
ES	−0.16	0.00	−1.03	0.97	−0.33	−0.12	−0.37	−0.24	−0.28	−0.22
MA	0.09	0.00	−0.77	0.80	−0.14	−0.12	−0.14	−0.24	−0.06	−0.21
MB	−0.95	0.00	−0.33	−0.15	−0.56	0.14	−0.72	0.26	−0.64	0.24
MC	−0.61	0.00	0.01	−0.21	−0.36	0.11	−0.40	0.18	−0.34	0.16
ME	−1.04	0.00	−0.66	0.16	−0.68	0.13	−1.08	0.50	−0.71	0.37
MO	−0.78	0.00	−0.26	−0.06	−0.47	0.11	−0.60	0.25	−0.52	0.22
NY	−3.96	0.00	−3.48	0.62	−2.70	0.43	−2.84	1.27	−2.33	1.30
PO	−0.85	0.00	−0.34	0.01	−0.52	0.12	−0.70	0.29	−0.56	0.25
ST	−0.76	0.00	−0.13	−0.20	−0.44	0.12	−0.56	0.22	−0.50	0.20
SU	0.26	0.00	−0.51	−0.58	−0.06	−0.09	0.08	−0.15	0.12	−0.13
SY	−2.85	0.00	−2.10	0.21	−2.10	0.08	−2.30	0.43	−2.07	0.32
VI	−0.59	0.00	−0.16	−0.09	−0.35	0.10	−0.44	0.19	−0.37	0.18
WE	−0.68	0.00	−0.18	−0.11	−0.41	0.11	−0.51	0.22	−0.44	0.19
WU	−0.46	0.00	−0.17	−0.39	−0.27	0.06	−0.31	0.12	−0.29	0.11

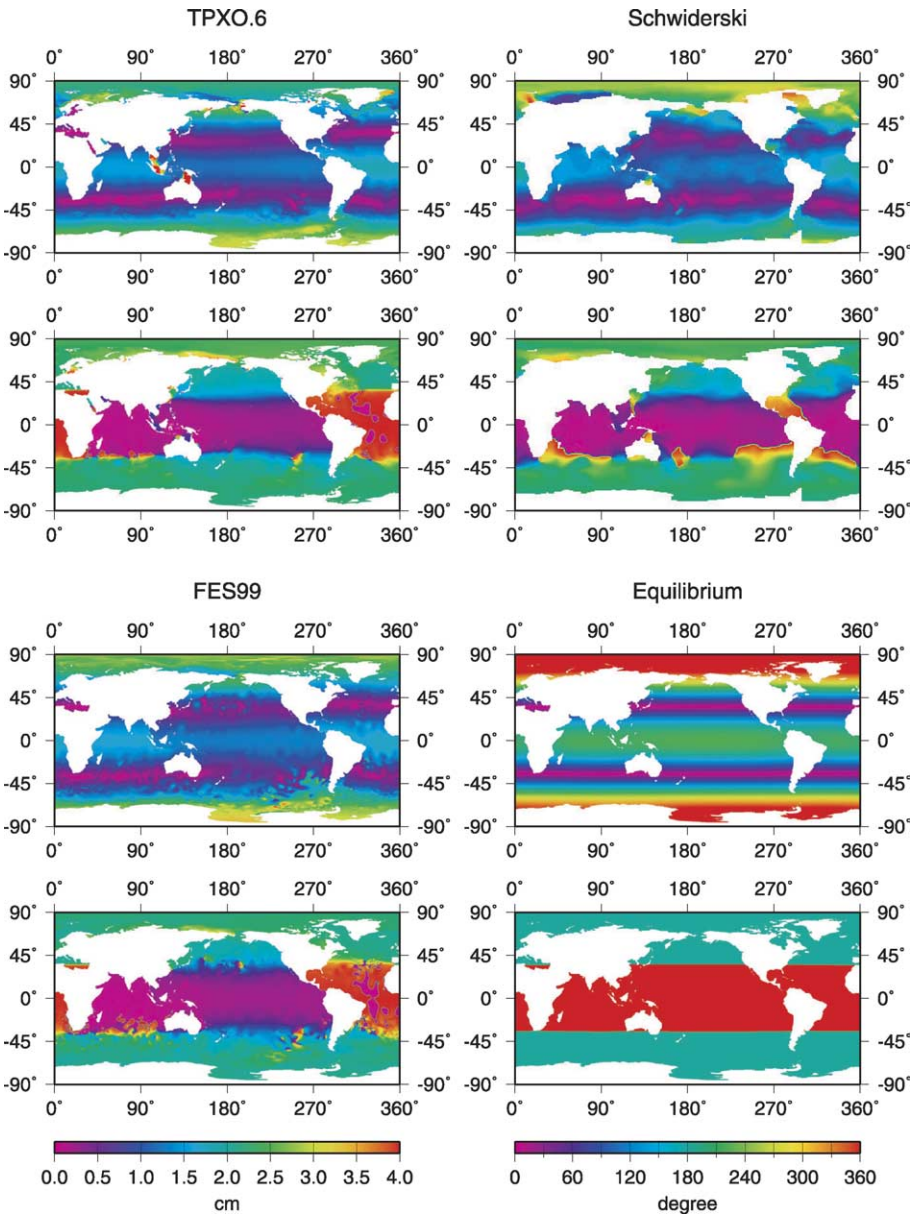

Fig. 1. Mf ocean tides according to FES99 (Lefèvre et al., 2002), TPXO.6 (Egbert and Erofeeva, 2002), Schwiderski (1980) and equilibrium models.

3. Processing of gravity data

3.1. Correction of gravity data

The raw minute gravity data for the 17 stations are corrected for major disturbances according to the classical method described by Crossley et al. (1993). Data are then decimated to a 1-day sampling using a finite-impulsive-response (FIR) low-pass filter, with a cut-off frequency of 0.33 cycle per day. The following main geophysical contributions are then corrected from the filtered gravity, by a simple subtraction:

- The polar motion and length-of-day induced effects are modeled using EOPC04 earth orientation parameters, assuming a static ocean response (Agnew and Farrell, 1978).

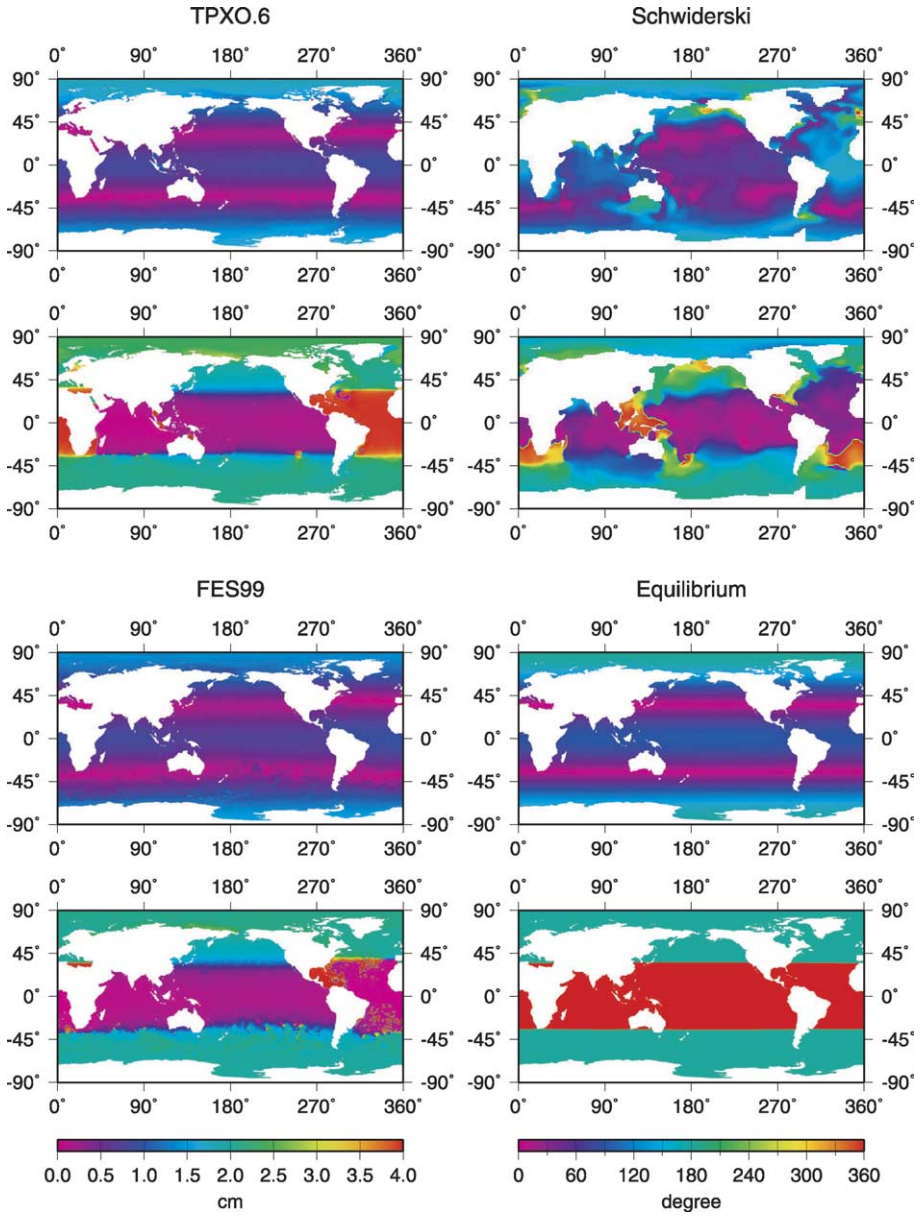

Fig. 2. Same as Fig. 1, but for Mm tidal wave.

- We model the atmospheric loading contribution by convolving the global surface pressure field provided by NCEP reanalysis (Kalnay et al., 1996) with the adequate Green's function (Boy et al., 2002) assuming an inverted barometer response of the ocean. This hypothesis has been shown to be valid for periods exceeding 10 days (Wunsch and Stammer, 1997; Egbert and Ray, 2003).

We choose not to correct gravity measurements for the hydrologic contributions as there is no significant and systematic reduction of gravity residuals by modeling the global soil-moisture and snow loading (see Boy and Hinderer, this issue).

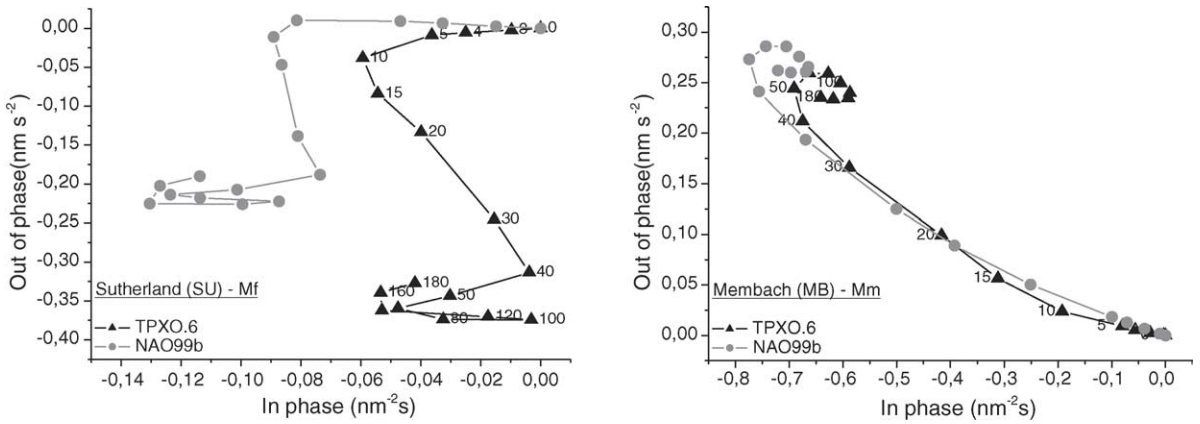

Fig. 3. Oceanic tidal loading as a function of the convolution domain, for two stations (Membach and Sutherland), two ocean models (TPXO.6 and NAO99b) and the two main long-period tides (Mf and Mm). 180° means a convolution over the whole Earth surface.

3.2. Tidal analysis

We first performed a tidal analysis of each corrected gravity data series (Wenzel, 1996). The observed amplitude and phase shift are then corrected for the solid Earth tidal contribution using Dehant et al. (1999) theoretical non-hydrostatic inelastic gravimetric factors and Hartmann and Wenzel (1995) tidal potential. Table 3 and Fig. 4 give the in-phase and out-of-phase components of the observed ocean tide loading for Mf and Mm tidal waves. For the Syowa instrument, we found comparable results with a previous study by Sato et al. (1997); however, although we analysed a longer time series (1225 days instead of 677 days), our error bars are significantly larger. This is possibly due to the fact that ETERNA software does not compute simple formal uncertainties but takes into account the noise level around the tidal frequencies.

The uncertainties of the Mm ocean tidal loading determination are usually quite large (i.e. of the order of magnitude of the loading signal itself or larger), except for very long records (such as Strasbourg or Membach) or for high latitude stations (Syowa and Ny Alesund), where the zonal tides are larger. Even if the uncertainties of Mf tidal wave are still large, they are almost always smaller than the loading contribution itself. We can notice that the observed Mf loading is coherent over for all the European stations. It is also worth mentioning that the contribution of Mf ocean tidal loading

Table 2
Same as Table 1, but for the fortnightly tide Mf

	Equilibrium		Schwiderski		FES99		NAO99b		TPXO.6	
	Real	Imaginary	Real	Imaginary	Real	Imaginary	Real	Imaginary	Real	Imaginary
BO	0.07	0.00	−0.15	−0.15	−0.01	−0.05	0.01	−0.10	0.04	−0.09
CA	−0.93	0.00	−0.72	−0.01	−0.27	0.35	−0.06	0.34	−0.06	0.35
CB	−0.65	0.00	−0.41	−0.02	−0.53	−0.11	−0.79	−0.08	−0.82	−0.09
ES	−0.38	0.00	−0.67	−0.08	−0.96	−0.21	−1.20	−0.29	−1.08	−0.49
MA	0.22	0.00	−0.29	−0.20	−0.60	−0.20	−0.74	−0.28	−0.66	−0.52
MB	−2.26	0.00	−1.39	−0.12	−1.11	0.41	−1.02	0.47	−0.86	0.42
MC	−1.44	0.00	−0.63	−0.13	−0.69	0.28	−0.53	0.24	−0.43	0.24
ME	−2.46	0.00	−1.16	0.40	−1.26	0.39	−1.37	1.20	−0.89	0.62
MO	−1.86	0.00	−1.05	−0.02	−0.91	0.33	−0.82	0.47	−0.67	0.37
NY	−9.48	0.00	−4.05	2.62	−5.00	1.27	−3.66	2.84	−2.88	1.99
PO	−2.02	0.00	−1.12	0.05	−1.00	0.35	−0.95	0.59	−0.73	0.41
ST	−1.80	0.00	−1.05	−0.14	−0.87	0.34	−0.75	0.38	−0.64	0.34
SU	0.62	0.00	−0.20	−0.05	−0.16	−0.34	−0.11	−0.19	−0.04	−0.33
SY	−6.78	0.00	−3.23	1.21	−4.10	0.70	−3.87	1.22	−3.53	1.22
VI	−1.40	0.00	−0.72	−0.01	−0.68	0.26	−0.57	0.35	−0.46	0.29
WE	−1.62	0.00	−0.88	−0.04	−0.79	0.30	−0.68	0.39	−0.56	0.32
WU	−1.09	0.00	−0.34	0.09	−0.42	0.13	−0.39	0.18	−0.43	0.27

Table 3
In-phase and out-of-phase components in nm s of the observed ocean tidal loading for Mm and Mf waves

SG stations	Analysed period	Mm			Mf		
		Real	Imaginary	Error	Real	Imaginary	Error
Boulder (BO)	199505–200310	0.09	0.03	0.39	0.12	−0.23	0.24
Cantley (CA)	199707–200310	0.00	−0.27	0.75	0.52	0.73	0.39
Canberra (CB)	199709–200112	−0.94	−0.13	0.45	0.26	−0.14	0.25
Esashi (ES)	199708–200212	0.44	0.05	1.02	−0.45	−0.16	0.49
Matsushiro (MA)	199707–200206	−1.52	−1.01	1.20	−0.62	−0.31	0.42
Membach (MB)	199609–200405	−0.72	0.06	0.41	−0.52	0.40	0.22
Medicina (MC)	199801–200402	−0.38	0.14	0.38	−0.41	0.11	0.18
Metsahovi (ME)	199409–200306	−0.51	0.76	0.84	−1.19	0.27	0.53
Moxa (MO)	200001–200403	−0.42	0.52	0.44	−0.34	0.39	0.19
Ny Alesund (NY)	199910–200207	−1.17	−1.43	1.56	−1.33	3.77	0.97
Potsdam (PO)	199408–199808	0.24	−0.07	0.45	−0.27	0.30	0.37
Sutherland (SU)	200004–200302	−0.69	0.14	0.49	−0.45	−0.12	0.21
Strasbourg (ST)	198708–199605	−0.86	0.91	1.31	−0.16	−0.07	0.55
	199703–200403	−1.25	−0.01	0.67	−0.14	0.28	0.36
Syowa (SY)	199707–200012	−2.48	0.33	2.30	−5.90	2.04	1.57
Vienna (VI)	199707–200401	−0.27	0.29	0.32	−0.26	0.41	0.17
Wettzell (WE)	199907–200312	0.32	−0.77	0.59	−0.54	0.75	0.27
Wuhan (WU)	199801–200312	−0.40	0.18	0.38	0.02	−0.38	0.29

For Strasbourg, two datasets are analysed from the former instrument GWR-T005, and the recent GWR CO26.

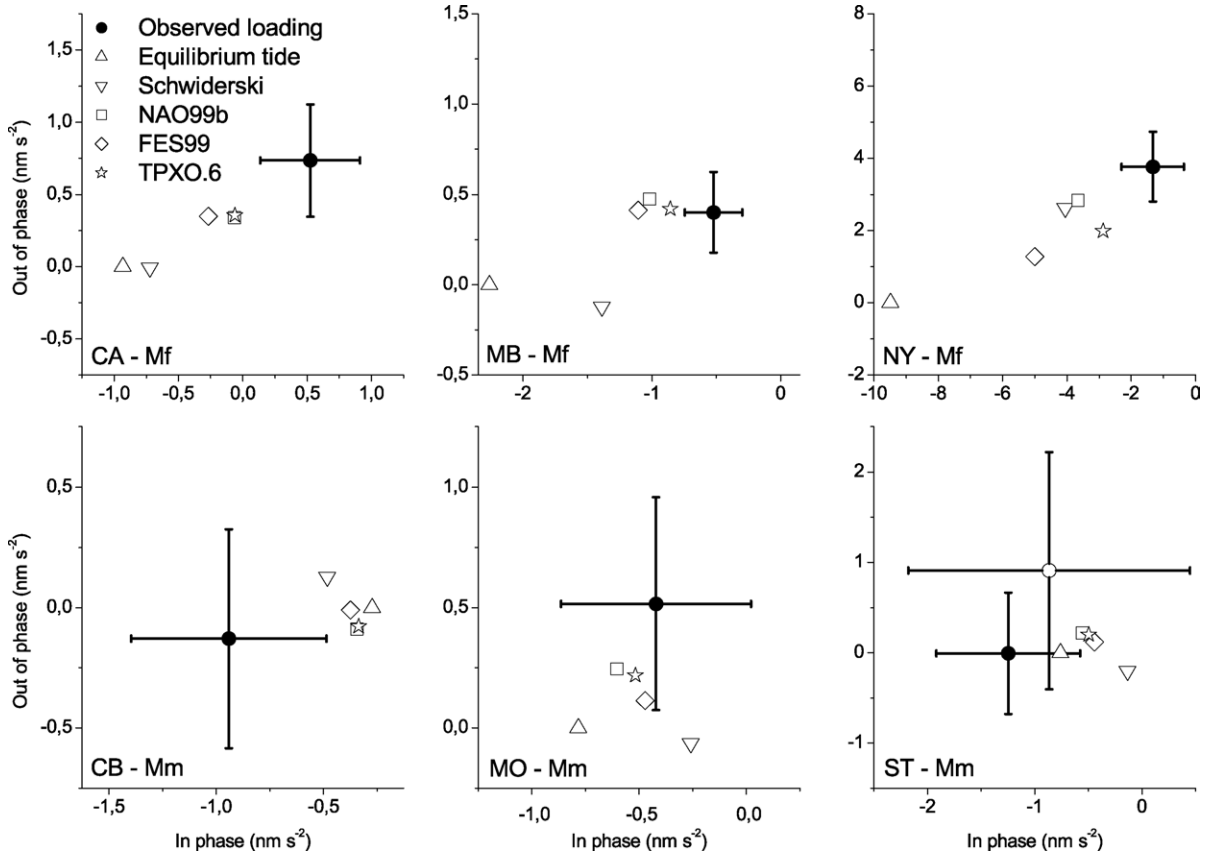

Fig. 4. Observed tidal loading for Mf (top) and Mm (bottom) waves and the estimated tidal loading for six gravimeters and the five models.

in Canberra is above the noise level, although this station is located near the node of the degree 2 Legendre polynomial. Therefore it is almost impossible to use up to now tidal gravity records to validate Mm ocean tidal models, but it may be possible for the fortnightly tide Mf.

4. Discussion and conclusion

In contrast to the major diurnal and semi-diurnal tides, the error bars of the estimated ocean tidal loading are quite large and significantly influenced by the long-term stability of the gravimeters (offsets, hydrologic contribution, etc.). It is really a problem for the estimation of the monthly tide loading effects, except for the high latitude stations (Syowa and Ny Alesund), or very long records (Strasbourg, Membach, for example). For almost all stations, it is possible to retrieve the fortnightly tide contribution; however we cannot differentiate the three recent tidal models with the superconducting gravimeters. However, recent models with assimilation of altimetry data and tide gauge data are significantly in better agreement with gravity tidal observations than the equilibrium tide or Schwiderski (1980) models.

A significant improvement of the determination of long-period ocean tide loading requires, at least, an estimation of the continental water storage changes (see Boy and Hinderer, this issue).

References

Agnew, D.C., Farrell, W.E., 1978. Self-consistent equilibrium ocean tides. Geophys. J. R. Astron. Soc. 55, 171–181.

Baker, T.F., Bos, M.S., 2003. Validating Earth and ocean tide models using tidal gravity measurements. Geophys. J. Int. 152, 468–485.

Bos, M.S., Baker, T.F., 2005. An estimate of the errors in gravity ocean tide loading computations. J. Geodesy 79, 50–63.

Bos, M.S., Baker, T.F., Rothing, K., Plag, H.P., 2002. Testing ocean tide models in the Nordic seas with tidal gravity observations. Geophys. J. Int. 150, 687–694.

Bos, M.S., Baker, T.F., Lyard, F.H., Zürn, W.E., Rydelek, P.A., 2000. Long-period lunar Earth tides at the geographic South Pole and recent models of ocean tides. Geophys. J. Int. 143, 490–494.

Boy, J.-P., Llubes, M., Ray, R., Hinderer, J., Florsch, N., Rosat, S., Lyard, F., Letellier, T., 2004. Non-linear oceanic tides observed by superconducting gravimeters in Europe. J. Geodyn. 38, 391–405.

Boy, J.-P., Llubes, M., Hinderer, J., Florsch, N., 2003. A comparison of tidal ocean loading models using superconducting gravimeter data. J. Geophys. Res. 108, doi:10.1029/2002JB002050.

Boy, J.-P., Gegout, P., Hinderer, J., 2002. Reduction of surface gravity data from global atmospheric pressure loading. Geophys. J. Int. 149, 534–545.

Crossley, D.J., Hinderer, J., Jensen, O.G., Xu, H., 1993. A slew rate detection criterion applied to SG data processing. Bull. Inf. Marees Terr. 117, 8675–8704.

Dehant, V., Defraigne, P., Wahr, J.M., 1999. Tides for a convective Earth. J. Geophys. Res. 104 (B1), 1035–1058.

Egbert, G.D., Ray, R.D., 2003. Deviation of long period tides from equilibrium: kinematics and geostrophy. J. Phys. Oceanogr. 33, 822–839.

Egbert, G.D., Erofeeva, S., 2002. Efficient inverse modeling of barotropic ocean tides. J. Atmos. Oceanogr. Technol. 19, 183–204.

Farrell, W.E., 1972. Deformation of the Earth by surface loads. Rev. Geophys. Space Phys. 10 (3), 751–797.

Hartmann, T., Wenzel, H.G., 1995. The HW95 tidal potential catalogue. Geophys. Res. Lett. 22 (24), 3553–3556.

Kalnay, E., Kanamitsu, M., Kistler, R., Collins, W., Deaven, D., Gandin, L., Iredell, M., Saha, S., White, G., Woollen, J., Zhu, Y., Chelliah, M., Ebisuzaki, W., Higgins, W., Janowiak, J., Mo, K.C., Ropelewski, C., Wang, J., Leetmaa, A., Reynolds, R., Jenne, R., Joseph, D., 1996. The NMC/NCAR 40-Year Reanalysis Project. Bull. Am. Meteorol. Soc. 77, 437–471.

Lefèvre, F., Lyard, F.H., Le Provost, C., Schrama, E.J.O., 2002. FES99: a global tide finite element solution assimilating tide gauge and altimetric information. J. Atmos. Oceanogr. Technol. 19, 1345–1356.

Matsumoto, K., Takanezawa, T., Ooe, M., 2000. Ocean tide models developed by assimilating TOPEX/POSEIDON altimeter data into hydrological model: a global model and a regional model around Japan. J. Oceanogr. 56, 567–581.

Richter, B., Wenzel, H.G., Zürn, W., Klopping, F., 1995. From Chandler wobble to free oscillations: comparison of cryogenic and other instruments in a wide period range. Phys. Earth Planet. Int. 91, 131–148.

Sato, T., Ooe, M., Nawa, K., Shibuya, K., Tamura, Y., Kaminuma, K., 1997. Long-period tides observed with a superconducting gravimeter at Syowa Station, Antarctica, and their implication to global ocean tide modeling. Phys. Earth Planet. Int. 103, 39–53.

Schwiderski, E.W., 1980. On charting global ocean tides. Rev. Geophys. Space Phys. 18 (1), 243–268.

Wenzel, H.G., 1996. The nanogal software: Earth tide data processing package ETERNA 3.30. Bull. Inf. Marees Terr. 124, 9425–9439.

Wunsch, C., Stammer, D., 1997. Atmospheric loading and the “inverted barometer” effect. Rev. Geophys. 35, 117–135.